European Journal of Radiology 83 (2014) 2260–2267

Contents lists available at ScienceDirect

European Journal of Radiology

journal homepage: www.elsevier.com/locate/ejrad

Analysis of decrease in lung perfusion blood volume with occlusive and non-occlusive pulmonary embolisms

Yohei Ikeda[a,*], Norihiko Yoshimura[a], Yoshiro Hori[d], Yosuke Horii[a], Hiroyuki Ishikawa[a], Motohiko Yamazaki[c], Yoshiyuki Noto[b], Hidefumi Aoyama[a]

[a] Department of Radiology, Niigata University Graduate School of Medical and Dental Science, Japan
[b] Department of Radiology, Niigata University Medical and Dental Hospital, Japan
[c] Department of Radiology, Niigata City General Hospital, Japan
[d] Department of Radiology, Showa University Fujigaoka Hospital, Japan

ARTICLE INFO

Article history:
Received 23 May 2014
Received in revised form 15 August 2014
Accepted 22 August 2014

Keywords:
Computed tomography
Angiography
Dual energy
Perfusion
Pulmonary embolism

ABSTRACT

Purpose: The aim of this study was to determine if lung perfusion blood volume (lung PBV) with non-occlusive pulmonary embolism (PE) differs quantitatively and visually from that with occlusive PE and to investigate if lung PBV with non-occlusive PE remains the same as that without PE.
Materials and methods: Totally, 108 patients suspected of having acute PE underwent pulmonary dual-energy computed tomography angiography (DECTA) between April 2011 and January 2012. Presence of PE on DECTA was evaluated by one radiologist. Two radiologists visually evaluated the PE distribution (segmental or subsegmental) and its nature (occlusive or non-occlusive) on DECTA and classified perfusion in lung PBV as "decreased," "slightly decreased," and "preserved". Two radiologists used a lung PBV application to set a region of interest (ROI) in the center of the lesion and measured HU values of an iodine map. In the same slice as the ROI of the lesion and close to the lesion, another ROI was set in the normal perfusion area without PE, and HUs were measured. The proportion of lesions was compared between the occlusive and non-occlusive groups. HUs were compared among the occlusive, non-occlusive, and corresponding normal groups.
Results: Twenty-five patients had 80 segmental or subsegmental lesions. There were 37 and 43 lesions in the occlusive and non-occlusive groups, respectively. The proportion of decreased lesions was 73.0% (27/37) in the occlusive group, while that of preserved lesions in the non-occlusive group was 76.7% (33/43). There was a significant difference in the proportion of lesions ($P < 0.001$) between the two groups. HUs of the iodine map were significantly higher in the non-occlusive group than in the occlusive group (33.8 ± 8.2 HU vs. 11.9 ± 6.1 HU, $P < 0.001$). There was no significant difference in HUs for the entire lesion between the non-occlusive (33.8 ± 8.2 HU) and corresponding normal group (34.5 ± 6.8 HU; $P = 0.294$).
Conclusion: Iodine perfusion tended to be visually and quantitatively preserved in lungs with nonocclusive PE. Lung PBV is required to evaluate pulmonary blood flow.

1. Introduction

Acute pulmonary embolism (PE) is a common disease with a high mortality rate [1]. The technical development of multidetector computed tomography (MDCT) has contributed to the detection of small embolisms in subsegmental pulmonary arteries. Therefore, MDCT has replaced scintigraphy and digital subtraction angiography as the first-line imaging tool for PE because of its high spatial resolution and short data acquisition time [2–4]. Lung perfusion blood volume (lung PBV) images are generated by dual-energy imaging and are used for the diagnosis of PE. Dual-energy imaging enables selective visualization of the iodine component in tissues on the basis of attenuation differences at different energy levels [5,6]. An image of lung PBV is a fusion of an iodine distribution image (iodine map) and a pulmonary computed tomography (CT) angiography (CTA) image. An iodine map is based on a three-material decomposition technique using iodine, air, and soft tissue [5]. Pulmonary dual-energy CTA (DECTA) does not expose patients to any significant additional radiation exposure compared with standard pulmonary CTA [7]. Perfusion defects in lung PBV are often not obvious in patients with non-occlusive lesions despite obvious PE observed on CTA [7,8]. One study on lung PBV reported that a

* Corresponding author. Tel.: +81 252272314.
E-mail address: ypfranky1@ybb.ne.jp (Y. Ikeda).

http://dx.doi.org/10.1016/j.ejrad.2014.08.015
0720-048X/

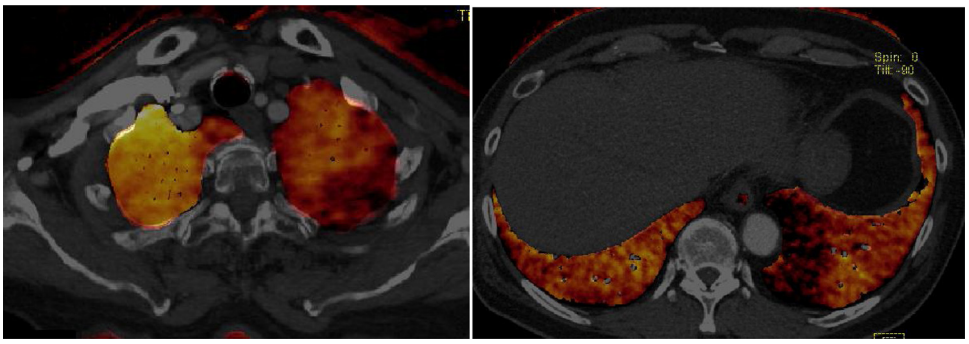

Fig. 1. Representative case of a "decreased" lesion and a "slightly decreased" lesion. The lesion in Lt. S1 + 2 is classified as "slightly decreased" (left). The lesion in Lt. S10 is classified as "decreased" (right).

corresponding perfusion defect was detected in 42 of 44 patients (95.5%) with occlusive PE, whereas only two of the 33 patients (6.1%) with non-occlusive PE were accompanied by a corresponding perfusion defect [7]. This study aimed to determine if lung PBV with non-occlusive PE differs quantitatively and visually from that with occlusive PE and to investigate if lung PBV with non-occlusive PE remains the same as that without PE.

2. Materials and methods

2.1. Patients

Our institutional review board approved this retrospective study, and informed consent was waived. Patient confidentiality was protected. Totally, 108 (35 men, 73 women; mean age, 62.2 ± 15.8 years; range, 12–88 years) patients with clinically suspected acute PE underwent DECTA between April 2011 and January 2012. The reasons for clinical diagnosis were acute chest pain, respiratory discomfort, and perioperative increase in D-dimer levels, among others. Patients with clinically suspected chronic PE based on clinical records were excluded.

2.2. CT imaging protocol

A dual-source CT scanner (Somatom Definition Flash; Siemens Medical Solutions, Forchheim, Germany) using the dual-energy mode was used to examine all patients. The following CT parameters were used: detector collimation, 2 mm × 64 mm × 0.6 mm; 330-ms rotation time; pitch, 0.55; and tube voltage, 140 kV and 100 kV. The tube current–time product varied for each patient. The slice thickness was set to 1.0 mm and the increment to 1.0 mm. For all images, a medium-soft convolution kernel (D30) was used. The mixed DECTA images equivalent to 120-kV images were reconstructed and obtained by deriving 40% of the image density from the 140-kV images and 60% from the 100-kV images.

On the basis of three-material decomposition of soft tissue, air, and iodine, iodine distribution images (iodine map) of the lung and lung PBV images were generated on a workstation (Syngo Acquisition Workplace; Siemens Medical Solutions, Forchheim, Germany). An image of lung PBV is a fusion of an iodine map and a pulmonary CTA image. The normalization of the window in the iodine map was performed by setting a region of interest (ROI) in the pulmonary artery trunk. The minimum CT value on the iodine map was −960, while the maximum CT value was −600. The range was set to 4 on a scale of 1–10.

A nonionic contrast medium (Iopamiron, 370 mgI/mL; Bayer Healthcare, Berlin, Germany) was administered at a flow rate of 0.06 × BW mL/s for 20 s. Then, a mixture of contrast medium and saline (1:1 ratio) was administered at the same rate. The scan was initiated using a bolus-tracking technique with an ROI placed over the pulmonary trunk, which triggered the scanner enhancement level of 250 HU. The trigger delay time was 10 s.

2.3. Analysis of DECTA images

The mixed DECTA images equivalent to 120-kV images were evaluated. We used a PACS system (Synapse; Fujifilm, Tokyo, Japan). The window level and window width were appropriately adjusted. At first, the presence of PE in DECTA was evaluated by one radiologist with 9 years of experience in cardiovascular imaging. Among all PE lesions, segmental or subsegmental lesions that did not extend to the proximal level were identified. Lesions that involved a shadow, such as pneumonia and atelectasis, were excluded.

Two radiologists with 9 (same as above) and 18 years of experience in cardiovascular imaging, respectively, independently evaluated segmental and subsegmental PE lesions. The PE distribution (segmental or subsegmental) and nature (occlusive or non-occlusive) were visually determined. When their original diagnosis did not concur, the radiologists discussed their decisions and reached a consensus diagnosis.

A non-occlusive lesion was defined when the lumen in the lesion (even if only slightly) and peripheral vessel exhibited contrast enhancement. An occlusive lesion was defined when both the lumen in the lesion and the peripheral vessel were not contrast enhanced. If the lesion extended over both the segmental and subsegmental branches, it was regarded as the segmental lesion.

2.4. Analysis of lung PBV images

Two radiologists (same as above) independently evaluated lung PBV. This analysis was performed 5 months after the analysis of DECTA to minimize the memory effect. The list of PE lesions without identifying their nature (occlusive or non-occlusive) in the DECTA images was used. The observers visually assessed only the lung PBV images without examining the DECTA images. The perfusion of the lesion was classified as "decreased," "slightly decreased," and "preserved" (Fig. 1). Classification was based on visual comparison with the normal perfusion area without PE in the same patient. If there were different interpretations of the lung PBV images, a final decision was determined by discussion, as conducted for analysis of the DECTA images.

Two radiologists with 9 (same as above) and 12 years of experience in cardiovascular imaging, respectively, independently measured the Hounsfield units (HUs). An ROI was set in the center of each lesion's perfusion area by using the lung PBV application of the workstation software (Syngo Acquisition Workplace; Siemens Healthcare), and HUs of the iodine map were measured. Furthermore, in the same slice as the ROI of the lesion and close to the lesion, another ROI was set in the normal perfusion area without PE,

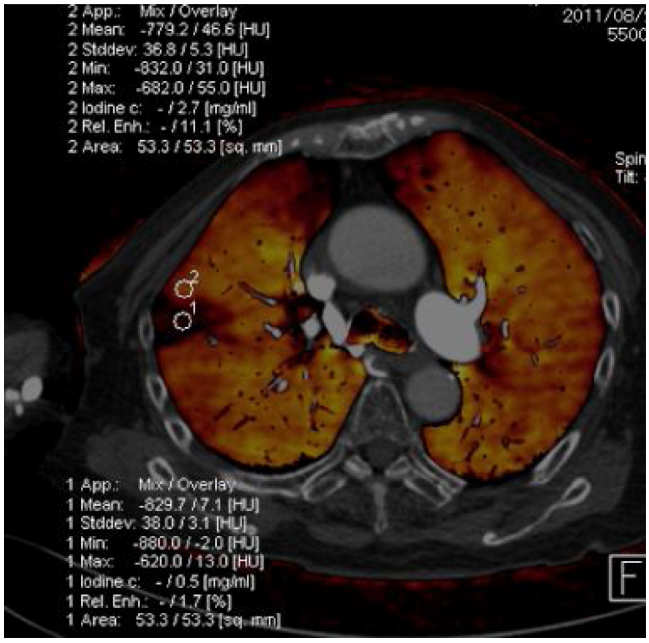

Fig. 2. Representative case for the measurement of HUs. An ROI was set in the center of the lesion's perfusion area using a lung PBV application, and HUs of the iodine map were measured. Furthermore, in the same slice and close to the lesion, an ROI was set in the normal perfusion area without PE, and HUs were measured.

and HUs were measured (Fig. 2). The ROI sizes were 50–100 mm^2 so as to not overlap the visible blood vessels. The measurements were performed once for each area. The mean HUs measured by the two radiologists was used for data analysis.

2.5. Data analysis

The chi-square test was performed to compare PE distribution between the occlusive and non-occlusive groups. Fisher's exact test was used to compare the proportion of lesions in the lung PBV images between the occlusive and non-occlusive groups. Student's *t*-test was used to compare HUs of the iodine map between the occlusive and non-occlusive groups. A paired *t*-test was used to compare HUs of the iodine map between the occlusive and non-occlusive groups and the corresponding normal group (normal perfusion area without PE). The proportion of lesions and HUs of the iodine map were separately compared in the entire lesion, the segmental lesion, and the subsegmental lesion. HUs were expressed as means ± standard deviation (SD). The interobserver variability in the interpretations of DECTA and lung PBV images was assessed using Cohen's kappa statistics. A κ value of >0.80 was defined as excellent agreement, 0.61–0.80 as good, 0.41–0.60 as moderate, 0.21–0.40 as fair, and <0.20 as poor. A *P*-value of <0.05 was considered statistically significant. A windows software (SPSS II; Nankodo, Tokyo, Japan) was used.

Table 1
PE distribution.

	Segmental	Subsegmental
Occlusive	18	19
37		
Non-occlusive	27	16
43		
Total	45	35
80		

With regard to PE distribution, there was no significant difference between the occlusive and non-occlusive groups ($P = 0.204$).

3. Results

3.1. Analysis of DECTA images

3.1.1. Patients and PE distribution

PE was observed in 38 of 108 (35%) patients, and all 38 patients were diagnosed with acute PE and treated with anticoagulant therapy, following which a clinical improvement was observed. Of these 38 patients, 13 were excluded; 11 patients had only PE lesions that extended to the proximal site and two had only peripheral PE lesions. The remaining 25 patients had 80 segmental or subsegmental lesions, which were evaluated for distribution and nature.

There were 37 lesions in the occlusive group and 43 lesions in the non-occlusive group (Table 1). With regard to PE distribution, there was no significant difference between the occlusive and non-occlusive groups ($P = 0.204$). There was excellent agreement on the PE distribution between the two reviewers ($\kappa = 0.85$; Table 2).

3.2. Analysis of lung PBV images

In the occlusive group, the proportion of decreased, slightly decreased, and preserved lesions was 73.0% (27/37), 27.0% (10/37), and 0%, respectively. In the non-occlusive group, the proportion of these lesions was 0%, 23.3% (10/43), and 76.7% (33/43), respectively (Table 3). There was a significant difference between the two groups in the proportion of lesions ($P < 0.001$). When compared separately, the proportion of decreased, slightly decreased, and preserved segmental lesions was 66.7% (12/18), 33.3% (6/18), and 0%, respectively, in the occlusive group and 0%, 29.6% (8/27), and 70.4% (19/27), respectively, in the non-occlusive group (Table 3). All these differences were significant between the two groups ($P < 0.001$). When compared separately, the proportion of decreased, slightly decreased, and preserved subsegmental lesions was 79.0% (15/19), 21.1% (4/19), and 0%, respectively, in the occlusive group and 0%, 12.5% (2/16), and 87.5% (14/16), respectively, in the non-occlusive group (Table 3). All these differences were significant between the two groups ($P < 0.001$). There was good agreement on the presence of perfusion decrease between the two reviewers ($\kappa = 0.73$; Table 4).

HUs of the iodine map were significantly higher in the non-occlusive group (33.8 ± 8.2 HU) than in the occlusive group (11.9 ± 6.1 HU; $P < 0.001$; Fig. 3). Similarly, even when the segmental and subsegmental lesions were separately compared, HUs

Table 2
Interobserver variability in interpretations of PE distribution.

	Observer 2				
	Occlusive segmental	Occlusive subsegmental	Non-occlusive segmental	Non-occlusive subsegmental	Total
Observer 1					
Occlusive segmental	15	2	2	0	19
Occlusive subsegmental	0	18	0	1	19
Non-occlusive segmental	0	0	27	3	30
Non-occlusive subsegmental	0	1	0	11	12
Total	15	21	29	15	80

$\kappa = 0.85$ excellent.

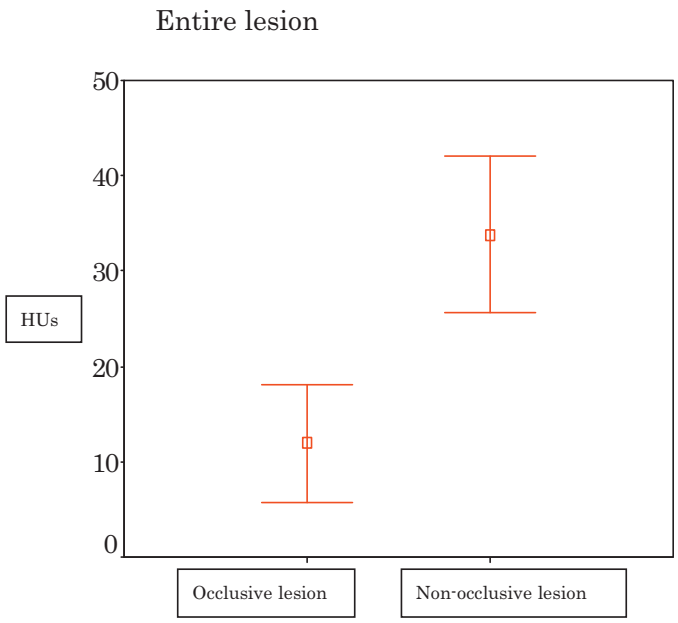

X-axis: lesion, Y-axis: HU
Occlusive lesion: 11.9 ± 6.1 HU (left)
Non-occlusive lesion: 33.8 ± 8.2 HU (right)
P < 0.001

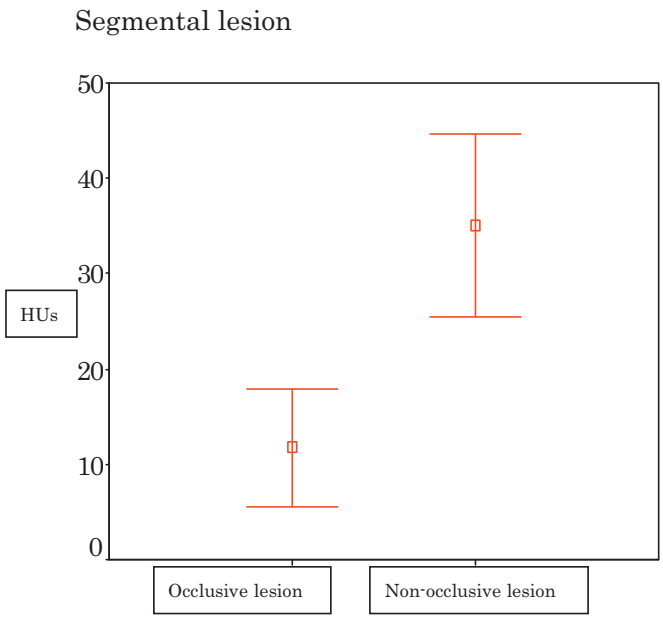

X-axis: lesion, y-axis: HU
Occlusive lesion: 11.7 ± 6.2 HU (left)
Non-occlusive lesion: 35.1 ± 9.6 HU (right)
P < 0.001

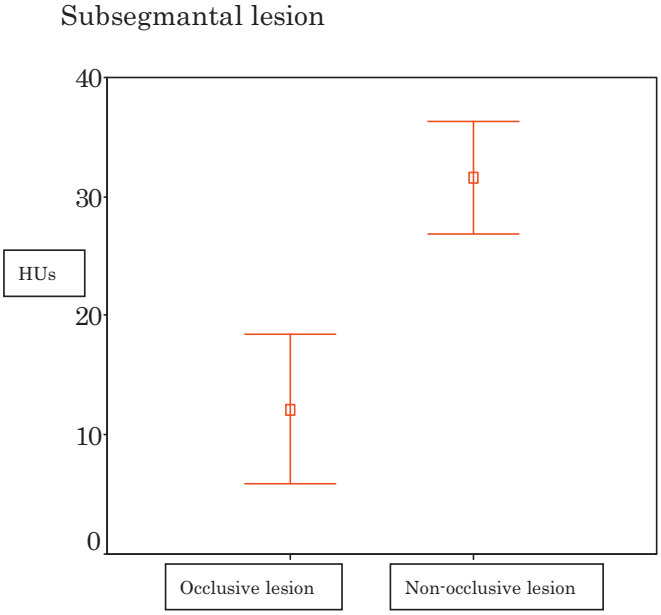

X-axis: lesion, y-axis: HU
Occlusive lesion: 12.2 ± 6.2 HU (left)
Non-occlusive lesion: 31.6 ± 4.7 HU (right)
P < 0.001

Fig. 3. Comparison between occlusive lesions and non-occlusive lesions on the basis of Hounsfield units (HUs) of the iodine map.

in the non-occlusive group were significantly higher (segmental lesions: 35.1 ± 9.6 HU vs. 11.7 ± 6.2 HU, respectively, $P < 0.001$; subsegmental lesions: 31.6 ± 4.7 HU vs. 12.2 ± 6.2 HU, $P < 0.001$; Fig. 3). HUs in the normal group were significantly higher than those in the occlusive group (entire lesion: 35.6 ± 6.3 HU vs. 11.9 ± 6.1 HU, respectively, $P < 0.001$; segmental lesions: 33.4 ± 5.7 HU vs. 11.7 ± 6.2 HU, respectively, $P < 0.001$; subsegmental lesions: 37.7 ± 6.3 HU vs. 12.2 ± 6.2 HU, respectively, $P < 0.001$; Fig. 4). There was no significant difference in HUs between the non-occlusive group and the corresponding normal group (entire lesion: 33.8 ± 8.2 HU vs. 34.5 ± 6.8 HU, respectively, $P = 0.294$; segmental lesions: 35.1 ± 9.6 HU vs. 35.9 ± 7.9 HU, respectively, $P = 0.389$;

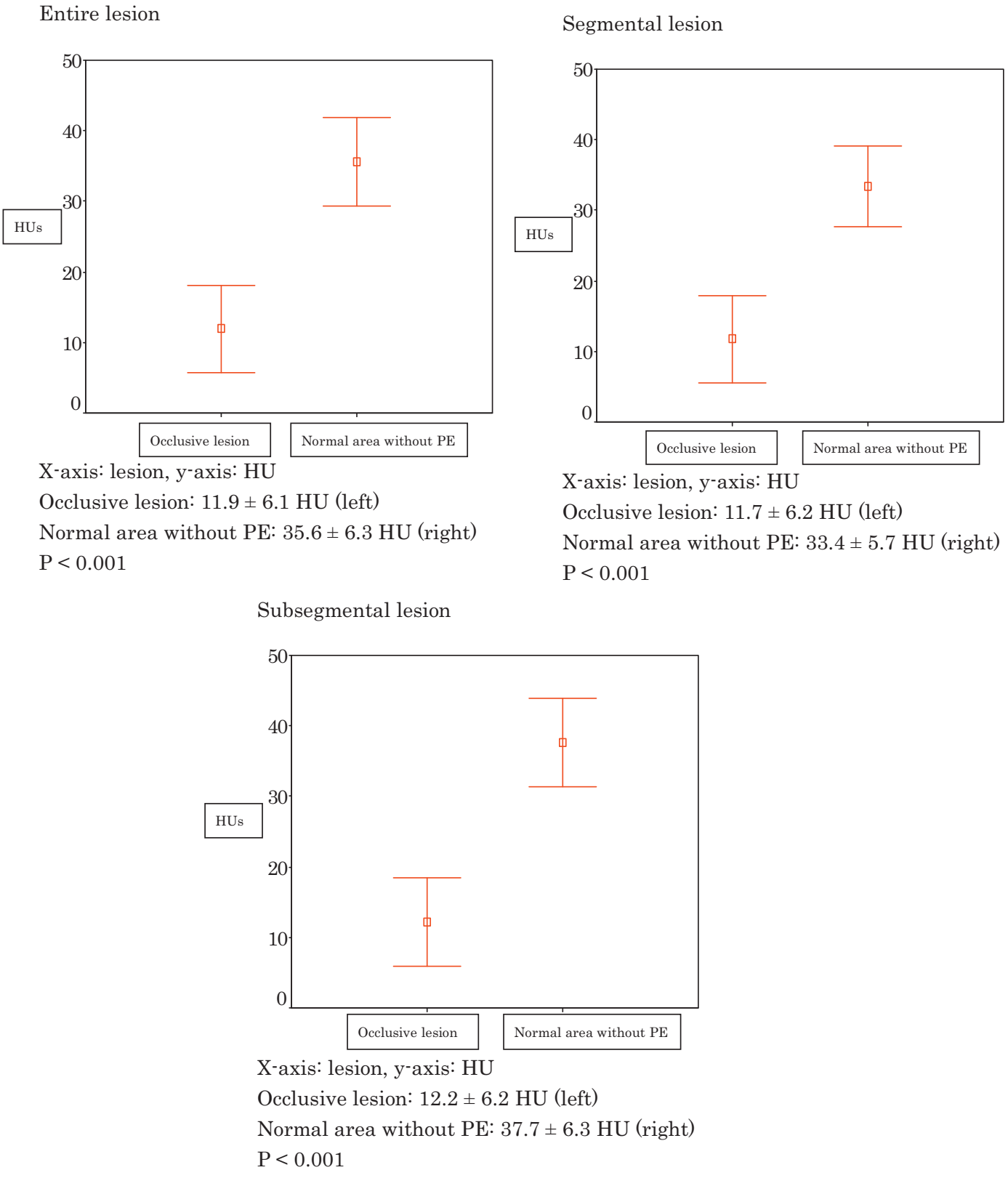

Fig. 4. Comparison between occlusive lesions and normal areas without PE lesions on the basis of Hounsfield units (HUs) of the iodine map.

subsegmental lesions: 31.6 ± 4.7 HU vs. 32.2 ± 3.5 HU, respectively, $P = 0.570$; Fig. 5).

Fig. 6 is a representative case with an occlusive lesion and a non-occlusive lesion.

4. Discussion

This study showed that iodine perfusion tended to be preserved in lungs with non-occlusive PE lesions. Previously, Thieme et al.

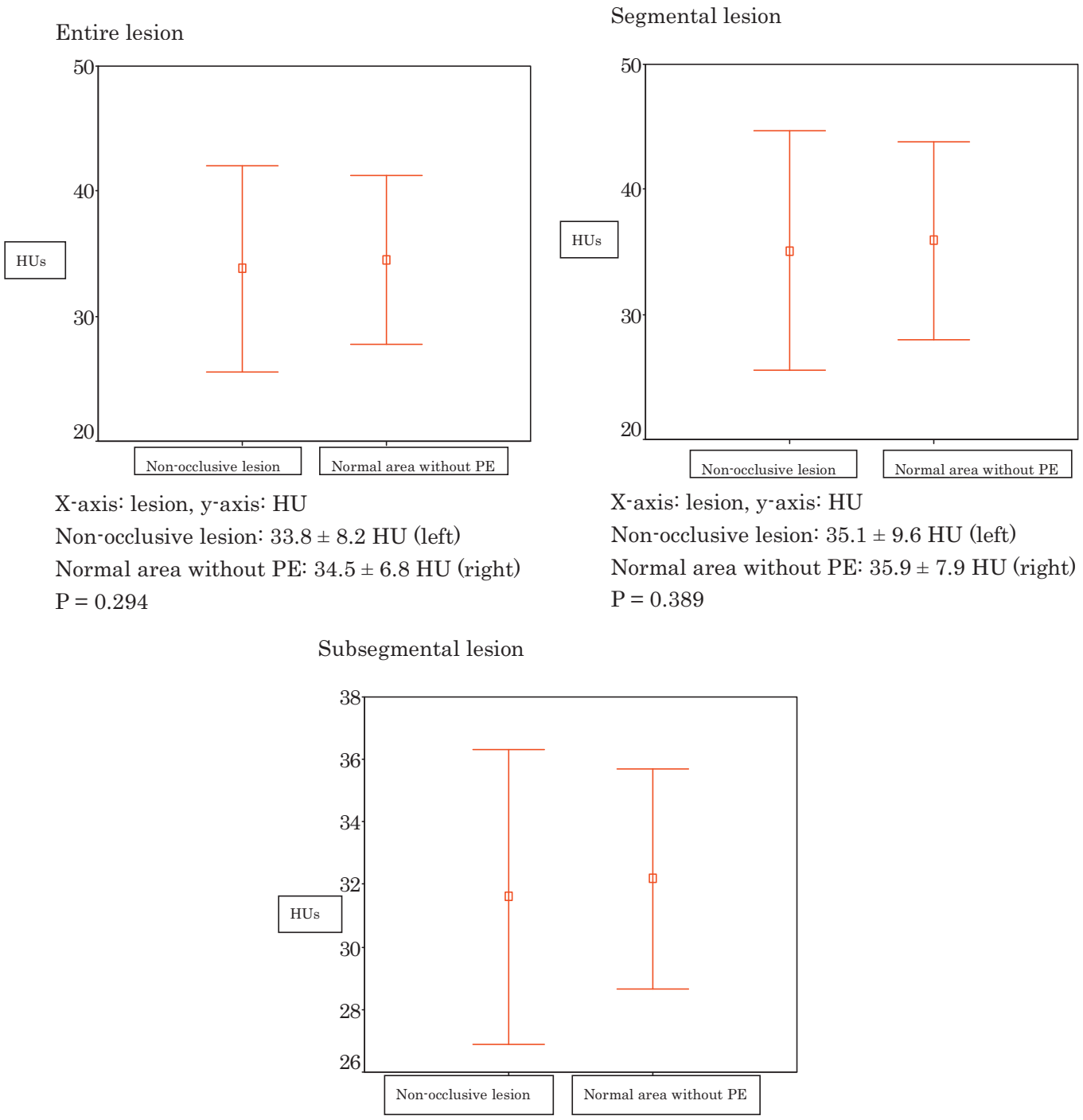

Fig. 5. Comparison between non-occlusive lesions and normal areas without PE lesions on the basis of Hounsfield units (HUs) of the iodine map.

[7] reported similar results that were visually verified. In addition to the visual evaluation, our study quantitatively confirmed preserved perfusion in lungs with non-occlusive PE by measuring HUs of the iodine map (Figs. 3–5). Hoey et al. [8] reported decreased attenuation values in partially occluded lobes in chronic PE. The novel approach taken in the present study was to measure the attenuation values (HUs) in acute PE and to evaluate the lesions in each segment or subsegment.

Our paper clarified that the degree of peripheral pulmonary blood flow could not be predicted by assessing only the presence or absence of PE on pulmonary CTA. Clark et al. [9] indicated that pulmonary artery patency assessments should be included in clot

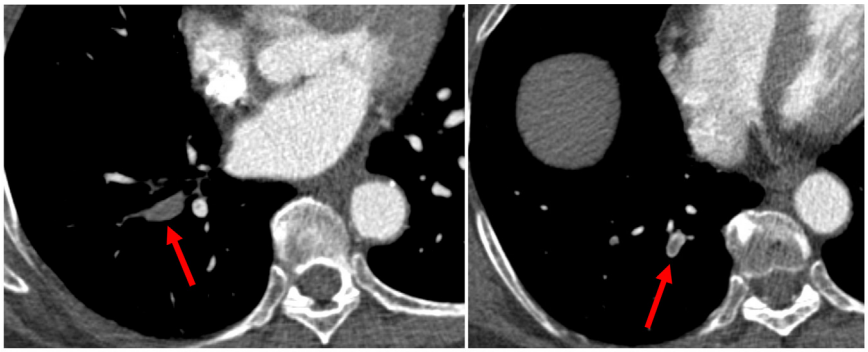

Rt. A9 has an occlusive PE lesion (left) and rt. A10 has a non-occlusive PE lesion (right).

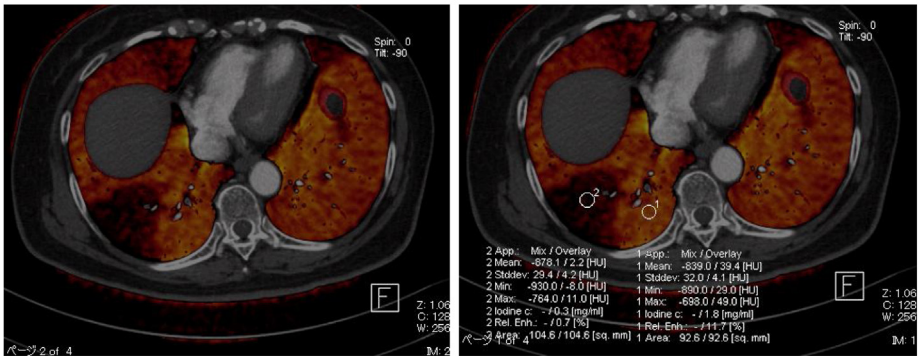

Fig. 6. Representative case with an occlusive lesion and a non-occlusive lesion. Lung PBV shows a wedge-shaped perfusion decrease in rt. S9. However, it is not seen in rt. S10. HUs of the iodine map are clearly different between rt. S9 and S10 (2.2 and 39.4, respectively).

load scores to improve their usefulness as predictors of PE severity. Our results with the lung PBV suggest that pulmonary artery patency is associated with the pulmonary vascular bed. If the pulmonary artery is small, a decision about patency may be difficult. Therefore, the lung PBV, which is likely associated with PE severity, is required to evaluate the pulmonary vascular bed.

Table 3
Analysis of lung PBV images.

	Decreased	Slightly decreased	Preserved
Entire lesion			
Occlusive 37	27 (73.0%)	10 (27.0%)	0
Non-occlusive 43	0	10 (23.3%)	33 (76.7%)
Total 80	27	20	33
Segmental lesion			
Occlusive 18	12 (66.7%)	6 (33.3%)	0
Non-occlusive 27	0	8 (29.6%)	19 (70.4%)
Total 45	12	14	19
Subsegmental lesion			
Occlusive 19	15 (79.0%)	4 (21.1%)	0
Non-occlusive 16	0	2 (12.5%)	14 (87.5%)
Total 35	15	6	14

In 'Entire lesion,' there was a significant difference between the occlusive and non-occlusive groups in the proportion of lesions ($P < 0.001$).
In 'Segmental lesion,' there was a significant difference between the occlusive and non-occlusive groups in the proportion of lesions ($P < 0.001$).
In 'Subsegmental lesion,' there was a significant difference between the occlusive and non-occlusive groups in the proportion of lesions ($P < 0.001$).

HUs in lung areas with non-occlusive PE did not significantly differ from those in lung areas without PE. This result indicates that peripheral blood flow from non-occlusive PE lesions is maintained as well as it is maintained in normal lungs. Therefore, it is clinically possible that lungs with non-occlusive PE lesions appear similar to normal lungs. This possibility, if true, can affect the therapeutic strategy.

Lung PBV images of normal patients in the supine position tend to show a posture-dependent gradient of iodine content [10]. HUs on normal lung PBV images vary depending on the location of the ROI. Furthermore, there may be a difference in the degree of contrast in the craniocaudal direction because there is a difference in the time phase of imaging. Therefore, in the present study, in the same slice as the ROI of the lesion and close to the lesion, another ROI was set in the normal perfusion area without PE (Fig. 2).

The proportions of slightly decreased lesions were 27% in the occlusive group and 23.3% in the non-occlusive group (Table 3). The reason for this difference is unclear, but the positions and sizes of the thrombi may have had an effect. Moreover, for the non-occlusive lesions, there appeared to be a greater influence from thrombus occlusions in the peripheral artery than from those in the subsegmental branch.

Table 4
Interobserver variability in interpretation of the lung PBV images.

	Observer 2			
	Decreased	Slightly decreased	Preserved	Total
Observer 1				
Decreased	26	5	0	31
Slightly decreased	3	10	1	14
Preserved	1	4	30	35
Total	30	19	31	80

$\kappa = 0.73$ good.

Previously, a study found that the sensitivity for peripheral PE detection was increased when lung PBV was used in addition to pulmonary CTA [5]. However, in that study, a distinction between the nature of PE lesions (occlusive or non-occlusive) was not performed. If limited to non-occlusive PE lesions, detection sensitivity should not increase in light of our results.

If appropriate treatment is not administered, acute PE can progress to chronic PE. Recently, pulmonary endarterectomy and percutaneous transluminal angioplasty (PTA) for chronic PE have been performed with improved outcomes [11–14]. Surgical treatment is performed for central PE. PTA is used to treat not only central PE but also peripheral PE. The effectiveness of pulmonary endarterectomy and PTA has been primarily evaluated using hemodynamic parameters (pulmonary arterial pressure and pulmonary vascular resistance) [11–14]. In addition, lung PBV may be a useful adjunct. Further investigation is needed.

Systemic collateral supply must be considered. In pulmonary CTA, chronic PE is more frequently associated with systemic collateral supply, such as that in the bronchial artery, than acute PE [15]. Because our study was intended to assess acute PE, it was not necessary to emphasize the impact of systemic collateral circulation. Our study results showed that there was a clear perfusion decrease in the occlusive lesions, but not in the non-occlusive lesions. Therefore, systemic collateral supply did not affect the differences in perfusion in the occlusive and non-occlusive lesions. However, it is possible that the perfusion decrease in both lesion types was underestimated by the systemic collateral supply.

Lung perfusion scintigraphy is another form of perfusion imaging. In our study, comparison with lung perfusion scintigraphy was not performed. Two studies have shown that dual-energy CT perfusion imaging was able to display pulmonary blood flow impairment with good agreement with scintigraphy findings [16,17]. It is possible that non-occlusive PE has been overlooked on scintigraphy when considering the results of this study. Unlike scintigraphy, lung PBV can simultaneously evaluate both thrombus and perfusion; therefore, pulmonary blood flow can be evaluated without anatomical mismatch.

This study had several limitations. First, it was a retrospective study. Second, it lacked an external reference standard for the correlation of results. We did not compare lung PBV with pulmonary perfusion magnetic resonance imaging and digital subtraction angiography. Third, we did not evaluate the relationship with the clinical severity of PE. Correlation between patency of the pulmonary artery and prognosis was also not evaluated. No clinical relevance for curative treatment of patients also was a major limitation in this study.

In conclusion, we used lung PBV to visually and quantitatively confirm that non-occlusive PEs are not associated with a decrease in blood flow compared with occlusive PEs and demonstrated a dissociation between pulmonary blood flow and thrombus distribution. In PE diagnosis, detection of a thrombus by CTA is essential. However, evaluation of pulmonary blood flow should be performed using lung PBV. The clinical relevance of the relationships among patency of the pulmonary artery, lung PBV, and patient outcomes needs to be further investigated.

Conflict of interest

The authors declared that there are no known conflicts of interest.

References

[1] Piazza G, Goldhaber SZ. Acute pulmonary embolism: Part I: epidemiology and diagnosis. Circulation 2006;114:28–32.
[2] Stein PD, Woodard PK, Weg JG, Wakefield TW, Tapson VF, Sostman HD, et al. Diagnostic pathways in acute pulmonary embolism: recommendations of the PIOPED II Investigators. Am J Med 2006;119:1048–55.
[3] Stein PD, Fowler SE, Goodman LR, Gottschalk A, Hales CA, Hull RD, et al. Multidetector computed tomography for acute pulmonary embolism. N Engl J Med 2006;354:2317–27.
[4] Wildberger JE, Mahnken AH, Das M, Kuttner A, Lell M, Gunther RW. Ct imaging in acute pulmonary embolism: diagnostic strategies. Eur Radiol 2005;15:919–29.
[5] Lee CW, Seo JB, Song JW, Kim MY, Lee HY, Park YS, et al. Evaluation of computer-aided detection and dual energy software in detection of peripheral pulmonary embolism on dual-energy pulmonary CT angiography. Eur Radiol 2011;21:54–62.
[6] Kang MJ, Park CM, Lee CH, Goo JM, Lee HJ. Dual-energy CT: clinical applications in various pulmonary diseases. Radiographics 2010;30:685–98.
[7] Thieme SF, Johnson TR, Lee C, McWilliams J, Becker CR, Reiser MF, et al. Dual-energy CT for the assessment of contrast material distribution in the pulmonary parenchyma. AJR Am J Roentgenol 2009;193:144–9.
[8] Hoey ET, Mirsadraee S, Pepke-Zaba J, Jenkins DP, Gopalan D, Screaton NJ. Dual-energy CT angiography for assessment of regional pulmonary perfusion in patients with chronic thromboembolic pulmonary hypertension: initial experience. AJR Am J Roentgenol 2011;196:524–32.
[9] Clark AR, Milne D, Wilsher M, Burrowes KS, Bajaj M, Tawhai MH. Lack of functional information explains the poor performance of 'clot load scores' at predicting outcome in acute pulmonary embolism. Respir Physiol Neurobiol 2014;190:1–13.
[10] Hagspiel KD, Flors L, Housseini AM, Phull A, Ali Ahmad E, Bozlar U, et al. Pulmonary blood volume imaging with dual-energy computed tomography: spectrum of findings. Clin Radiol 2012;67:69–77.
[11] Fedullo P, Kerr KM, Kim NH, Auger WR. Chronic thromboembolic pulmonary hypertension. Am J Respir Crit Care Med 2011;183:1605–13.
[12] Mizoguchi H, Ogawa A, Munemasa M, Mikouchi H, Ito H, Matsubara H. Refined balloon pulmonary angioplasty for inoperable patients with chronic thromboembolic pulmonary hypertension. Circ Cardiovasc Interv 2012;5:748–55.
[13] Kataoka M, Inami T, Hayashida K, Shimura N, Ishiguro H, Abe T, et al. Percutaneous transluminal pulmonary angioplasty for the treatment of chronic thromboembolic pulmonary hypertension. Circ Cardiovasc Interv 2012;5:756–62.
[14] Andreassen AK, Ragnarsson A, Gude E, Geiran O, Andersen R. Balloon pulmonary angioplasty in patients with inoperable chronic thromboembolic pulmonary hypertension. Heart 2013;99:1415–20.
[15] Hong YJ, Kim JY, Choe KO, Hur J, Lee HJ, Choi BW, et al. Different perfusion pattern between acute and chronic pulmonary thromboembolism: evaluation with two-phase dual-energy perfusion ct. AJR Am J Roentgenol 2013;200:812–7.
[16] Thieme SF, Becker CR, Hacker M, Nikolaou K, Reiser MF, Johnson TR. Dual energy CT for the assessment of lung perfusion—correlation to scintigraphy. Eur J Radiol 2008;68:369–74.
[17] Thieme SF, Graute V, Nikolaou K, Maxien D, Reiser MF, Hacker M, et al. Dual energy CT lung perfusion imaging—correlation with SPECT/CT. Eur J Radiol 2012;81:360–5.